International Journal of Advances in Applied Sciences (IJAAS)
Vol. 15, No. 3, Sept 2026, pp. 932~943
ISSN: 2252-8814, DOI: 10.11591/ijaas.v15.i3.pp932-943

Multilevel local region sparse shape composition model for liver cancer classification

Balasubramanian Sakthisaravanan[1], Ramakrishnan Meenakshi[2], Thirugnanasambandam Akila[3], Saravanan Durga Devi[4], Subbiah Murugan[5]
[1]Department of Computer Science and Engineering, Sri Venkateshwara College of Engineering, Bengaluru, India
[2]Department of Computer Science and Engineering, Chennai Institute of Technology, Chennai, India
[3]Department of Information Technology, Mahendra College of Engineering, Salem, India
[4]Department of Computer Science and Engineering, Vel Tech High Tech Dr. Rangarajan Dr. Sakunthala Engineering College, Chennai, India
[5]Department of Biomedical Engineering, Saveetha School of Engineering, Saveetha Institute of Medical and Technical Sciences, Saveetha University, Chennai, India

Article Info

Article history:

Received May 17, 2025
Revised Jun 3, 2026
Accepted Jun 17, 2026

Keywords:

Computed tomography
Liver cancer
New multi-support vector machine
Novel multilevel local region-based sparse shape composition
Shape composition model

ABSTRACT

Machine learning and computer-assisted disease detection are two technological innovations that have significantly improved medical advancement, and recent research has demonstrated their effectiveness. Liver cancer is one of the important causes of cancer-related deaths internationally. Tumor detection in the liver and its classification is challenging due to poor accuracy and high processing requirements available in the existing techniques. In these, there is a loss of edge information and the quality of the images considered. To address these issues in the segmentation and classification of liver cancer, a novel feature extraction method and algorithm called the novel multilevel local region (MLR)-based sparse shape composition model (NMLR-SSC) were developed. This innovative technique identifies the existence of tumors on abdominal computed tomography (CT) images. The input images were obtained from the 3D-IRCADb-01 dataset. The algorithm showed an improvement of 0.22%. When compared to other classifiers. The proposed algorithm showed 100% specificity, sensitivity, and a 98% accuracy rate in detecting the liver tumor.

Corresponding Author:

Balasubramanian Sakthisaravanan
Department of Computer Science and Engineering, Sri Venkateshwara College of Engineering
Bengaluru, Karnataka, India
Email: sakthisaravanan.b_cy@svcengg.edu.in

1. INTRODUCTION

Liver cancer is among the main causes of cancer-related mortality globally, with early identification being vital for enhancing patient survival rates. Despite advancements in imaging technology such as computed tomography (CT), the precise diagnosis and categorization of liver tumors continue to be problematic due to tumor heterogeneity, indistinct margins, and variability across patients. Recent advancements in machine learning and sparse representation methodologies have shown potential in overcoming these issues by effectively capturing discriminative characteristics and minimizing duplicate information. This research introduces a novel multilevel local region (MLR)-based sparse shape composition (NMLR-SSC) model integrated with a new multi-support vector machine (NMSVM) for the identification and classification of liver tumors, motivated by existing limitations. To classify CT scans as either having a tumor (hepatocellular or metastatic) or not, this research introduces a novel deep learning (DL) model,

U-Net70, for liver tumor classification [1]. Building a deep learning system (DLS) using convolutional neural networks (CNNs) to categorize liver tumors using a combination of clinical data, including text and laboratory test results, and enhanced and unenhanced magnetic resonance imaging (MRI) [2]. Histological images connected with liver cancer differentiation were compared using the region-based convolutional neural network (R-CNN) DL algorithm in a research [3]. To improve the efficiency of liver and tumor segmentation, this research proposes an advanced method that combines Gabor features (GF) with three separate machine learning algorithms: random forest (RF), support vector machine (SVM), and deep neural networks (DNN) [4]. To ensure uniformity and consistency among CT liver slices, GF-based texture data is meticulously created. Classifying liver disorders from ultrasound images, which attempts to solve problems with segmentation, features, and parameter combinations [5].

An optimization-driven strategy is used by the liver segmentation and classification model, which pre-processes, segments, extracts features from, and classifies CT images [6]. This research presents a CNN-based automated method for CT scan liver and tumor segmentation [7]. With the 3D-IRCADb dataset, the system uses U-Net and a modified residual U-Net to preserve spatial information while extracting features. In order to classify liver cancer from CT images, a novel method that integrates pre-processing, segmentation, feature extraction, and classification [8]. An improved method for detecting liver diseases in developing nations is presented in this article [9]. It uses a customized mask-region CNN (CM-RCNN) for deep liver segmentation and classification. Segmentation, feature extraction, and adaptive histogram equalization are all used by the system to improve accuracy. Using residual U-Net (ResU-Net), a hybrid DL network, a DL model is applied to CT images to segment tumors and livers [10]. This work presents a new approach to early liver disease identification utilizing non-contrast CT scans to distinguish between tumors, adverse events, and healthy patients [11]. The proposed solution incorporates a CNN-based classification framework after an RCNN-based automated liver area identification procedure. Used MRI of the liver to create an automated deep classification system that could identify cancer [12]. Adaptive thresholding, local binary patterns, bilateral deep filtering, and a pre-trained ResU-Net Architecture model are all used by the system. This is achieved by combining the feature extraction capabilities of CNN with the classification efficiency in high-dimensional spaces of SVM [13]. An architecture for MRI-based liver cancer detection utilizing CNN integrates Bayesian optimization and long short-term memory (CNN-BO-LSTM) [14]. The current study introduces a fresh and efficient approach to extracting liver tumors from publicly available CT scans by combining ResNet and U-Net models [15]. Implementing a residual squeeze-excited U-Net architecture, a self-attention-based deep convolutional adaptive capsule network, and extended gannet optimization for successful classification for segmenting and categorizing liver cancer illness [16].

This study uses several DNNs for the purpose of segmenting and classifying liver tumor diseases [17]. The research used improved probabilistic neural networks (IPNN)-BO to segment liver tumors using CT scan images for the best possible categorization [18]. The innovative use of the R-CNN algorithm in DL to accurately classify histological images linked to liver cancer, which differentiates it [3]. Using CT images and pathology data to forecast liver cancer variations and metastasis proposes a DNN for multi-class malignant liver diagnosis [19]. To classify liver cancer variations, the network learns five pathogenic characteristics and combines downscaled hierarchical features. Using a DL-based hybrid CNN model, this research introduces a novel approach to automatically segmenting and classifying liver tumors [20]. An objective prediction of liver tumors is the goal of the approach. A deep CNN, a new tool for automatically segmenting and classifying hepatic tumors in CT scan images [21]. Developed a modified Dense U-Net model specifically for tumor segmentation. The method described in this study uses a combination of a fully connected layer, four Chebyshev graph convolution layers, and a unique DL approach to properly segment the liver and liver tumors in CT maps [22]. A computerized approach for automatic segmentation of hepatic tumors using MRI and CT scans, with layered thresholding and electromagnetic optimization for faster and more accurate results [23]. Liver cancer is a deadly malignant tumor, and this paper looks at how DL approaches have been used to analyze multimodal fusion image segmentation for this disease [24]. To provide thorough and accurate segmentation, it talks about using DL approaches like U-Net and CNN. The artificial neural network (ANN) model distinguishes between normal and malignant diseases efficiently [25].

2. PROPOSED WORK

This section deliberates the implementation details of the NMLR-SSC-MSVM technique. All the work is implemented in MATLAB. Figure 1 furnishes the proposed system workflow. Preprocessing removes the noisy region from the input abdominal CT images with an adaptive median filter. Subsequently, the hybrid image segmentation framework (HISF) is performed based on the NMLR-SSC to segment the liver image from the preprocessed CT image and then segment the tumor part. The next stage extracts features using hybrid statistical features with grey level co-occurrence matrix (HSGLCM).

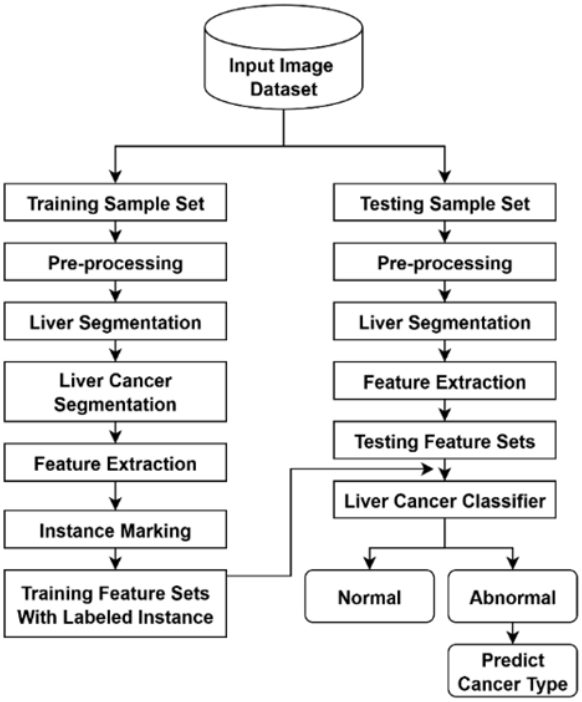

Figure 1. Proposed NMSVM workflow

After extracting the features, instance marking is enabled to effectively label the instances in the training sample set, such as 0, 1, 2, 3, 4, 5, 6, and 7, respectively. In that case, seven types of liver cancer identification are labelled. In the runtime testing stage, the same preprocessing, segmentation, and feature extraction techniques are enabled. To obtain the testing feature sets. An NMSVM classifier helps to automate the entire process. The novelty involves combining multilevel local area decomposition with SSC, enabling accurate edge preservation and reliable tumor characterization, validated by clinical-grade specificity, sensitivity, and accuracy metrics for liver cancer classification. The NMLR-SSC framework is a technique for the analysis of liver images. It has four primary stages: area segmentation, feature extraction, sparse dictionary generation, and classification approach. CT scans undergo pre-processing to reduce noise and standardize intensity values, followed by a multilevel local area decomposition to segment the liver image into hierarchical sub-regions. Sparse coding minimizes repetition and ensures that only relevant shape components impact classification. The sparse shape vectors are then fed into an NMSVM classifier, which establishes appropriate decision boundaries and ultimately categorizes each area as tumor-positive or tumor-negative.

2.1. Image preprocessing

The preprocessing is performed based on the adaptive median filter to dispose of the noisy pixels from the liver image. Smoothening impacts are decreased. The filtering coefficient is supplemented with noisy pixels to enhance the nature of the information image pixel. Reduce distortion, the method spares the edge points of interest of the image during preprocessing. Commotions in an image are grouped into settled and irregular frequency noise. The settled esteem clamors are the spike commotions, and the estimation of the tainted pixels will be either equivalent to zero or 255 with a square with the likelihood (p/2). The arbitrary esteemed motivation commotion will have the tainted pixel values consistently conveyed between 0 and 255. The dim scale image contains the values [0, 255]. The way to expel noise from the image is accomplished by looking at the force estimations of each pixel with the neighboring pixels. To achieve this, a 3×3 window is shaped, and it is made to slide on the image.

2.2. Image segmentation framework

The image segmentation is established into two main processes, the NMLR-SSC. Here, a set of S_n corresponding triangular liver training shapes $\{T_i | i = 1, 2, \dots, s_n\}$ and an individual shape T_i in terms of shape vector $v_i = \left(d_{i1}^M d_{i2}^M, \dots, d_{il_p}^M\right)^M$, where $d_{ij} = r_{ij}, c_{ij}$ represents the jth point of shape T_i, and l_p is

denoted as the number of landmark focuses. At that point, spatially adjusting all training shapes into a typical organized outline utilizing the calculation, the mean liver shape $\bar{T}$ can be called the shape vector. It's shown as in (1).

$$\bar{v} = \left(\gamma_1^M, \gamma_2^M, \dots, \gamma_{lp}^M\right)^M = \sum_{I=1}^{S_n} \frac{v_i}{S_n} \quad (1)$$

2.2.1. Multilevel shape division

In a multilevel manner, the different regions are acquired from the disintegration consequences of liver shapes, so that every area has homogeneous shape variety. Overall, the standard deviation of the training shapes' positions at first glance is inferred as the shape variety of the n^{th} landmark point, as demonstrated in (2).

$$S.D_i = \sqrt{\frac{1}{s_n - 1}} \sum_{k=1}^{S_n} \|d_{ki} - \gamma_i\|_2^2 \quad (2)$$

2.2.2. Novel multilevel local region-based sparse shape composition

The hybrid segmentation method of the MLR method is utilized to segment the liver portion firstly from the overall abdomen CT image, and then the SSC method is utilized to segment the cancer portion. Initially, the pixels' presence in the CT scan image is around the liver. Based on that image, the index value forms a region with the help of neighboring pixels. This formation method is named the MLR model. For an individual region, the multilevel neighborhood repository is formed based on the detection of multilevel shape division with a homogeneous shape vector. Vector $v_{lj}^i \in (\mathbb{R}^{3n_1})$ where n_1 represents the quantity of apexes of the province at level *l*, which is employed to represent the pre-adjusted T_{lj}^i through the connection of the coordinates of all its vertices. From that point onward, the shape vectors indicating the comparative jth regions at level *l* are loaded as individual *j*. This makes a neighbourhood pixel value for jth region at level *l*: $T_{lj} = \left[T_{lj}^1, T_{lj}^2, \dots, T_{lj}^k\right] \in \mathbb{R}^{3n1 \times K}$, where K denotes the quantity of the preparation stage. The general liver origin shape at level l, T_l, is named as the connection of all the border exact liver shape depositories, as in (3).

$$T_l = \left[T_{l1}, T_{l2}, \dots, T_{ln_l}\right] \in \mathbb{R}^{(3_{nl \times K}) \times n_l} \quad (3)$$

Afterwards, the shape is obtained by utilizing the NMLR model. A multilevel shape division is obtained by proliferating the shape separation features with the mean liver texture. The input shape at level l can then be represented by a shape vector as in (4).

$$v_l = \left[v_{l1}, v_{l2}, \dots, v_{ln_l}\right] \in \mathbb{R}^{(3_{nl \times K}) \times n_l} \quad (4)$$

2.2.3. Sparse shape representation

Decompose the provided CT image into localized sections $R = \{r_1, r_2, \dots, r_n\}$. Each area r_i is denoted as a feature vector $x_i \in \mathbb{R}^d$ can be estimated by a sparse linear combination of basis atoms from a dictionary $D \in \mathbb{R}^{d \times k}$. Where $\alpha_i \in \mathbb{R}^k$ is the sparse coefficient vector.

$$x_i \approx D\alpha_i \quad (5)$$

2.2.4. Objective function

The sparse coding problem is formulated as in (6).

$$\min_{\alpha_i} \| x_i D\alpha_i \|_2^2 + \lambda_1 \| \alpha_i \|_1 + \lambda_2 \Omega(\alpha_i) \quad (6)$$

Where $\| x_i - D\alpha_i \|_2^2$ is reconstruction error (ensures features can be expressed via dictionary atoms), $\| \alpha_i \|_1$is ℓ_1-norm sparsity constraint (encourages few active atoms, reducing redundancy), $\Omega(\alpha_i)$ is structural regularization term that preserves shape continuity and edge boundaries, and λ_1, λ_2 is regularization weights balancing sparsity vs. structure preservation.

2.2.5. Optimization method

The problem is convex and addressed using the iterative shrinkage-thresholding algorithm (ISTA) or its faster iterative shrinkage-thresholding algorithm (FISTA) variant. The steps for updating are as shown in (7).

$$\alpha_i^{(t+1)} = S_{\lambda/L}\left(\alpha_i^{(t)} - \frac{1}{L}D^T(D\alpha_i^{(t)} - x_i)\right) \quad (7)$$

2.2.6. Classification integration

Once sparse codes α_i are collected, they are used as input for an NMSVM.

$$\min_{w,b}\frac{1}{2}||w||_2^2 + C\sum_{i=1}^{n} max(0,1 - y_i(w^T\alpha_i + b) \quad (8)$$

Where $y_i \in \{-1,+1\}$ denotes class labels (tumor/non-tumor), w, b are classifier parameters, and C is a penalty parameter controlling margin violation. The final decision rule is in (9).

$$f(\alpha_i) = sign(w^T\alpha_i + b) \quad (9)$$

Then, the resultant segment image of a liver is given to the SSC model, which segregates the cancer portion. In this scheme, the algorithm is performed based on two sparsity properties. Primarily, derive the linear combination of the shape vectors. Then, secondarily, convert the binary form of the pixel into a color image, which reduces the gross errors.

2.3. Feature extraction

The feature extraction process is applied to remove the relevant and informative features, also known as dimensionality reduction. It is named the HSGLCM model. The segmented tumor includes measures such as standard deviation, mean, energy, kurtosis, skewness, and entropy. Then, the grey level co-occurrence matrix (GLCM) model is applied to characterize the texture features, and it calculates the scalar values of the image. The extracted features are mainly based on the 12 statistical features that have been created by using the HSGLCM model.

The main aim of the classification step is i) to differentiate cancerous or non-cancerous cells and ii) to categorize different subtypes of these tumor cells ranging from 0 to 7. The 0 value characterizes the dark region of the tumor, which is said to be a normal region, and the otherwise white portion of the image is classified into 1 to 7 tumor types. The main involvement of using NMSVM is i) unlabeled data allows us to improve predictive models, ii) minimizes redundancy, and iii) it speeds up the learning tasks and reduces labelling costs. The NMSVM classifier achieves a separate surface from the input space of the dataset, which utilizes a different kernel occupation, such as linear or nonlinear, such as "quadratic", "polynomials", and the "radial basis functions (RBF)". There are a total of 8 classes in the form of binary classification range: [0, 7]. Initially, the training and testing features are given to the classification model as input. The mean value of the train and test features is derived, and then the exponential probability density function of the train and test images is estimated.

2.4. Experimental results

The analyses were carried out using the 3D-IRCADb-01 dataset, including 3D CT scan volumes obtained from 10 individuals. Approximately 75% of the patients have hepatic tumors, making the dataset very relevant for clinical tumor investigation. Each patient file contains many CT slices ("liver_numéro.jpg"), along with license and credit information. The collection provides high-resolution abdomen CT images that enable region-level segmentation and tumor identification.

The NMLR-SSC method first uses multilayer local area decomposition on the CT images, maintaining complex edge patterns and localized intensity fluctuations. This stage ensures the preservation of tumor borders, which are often indistinct in traditional segmentation techniques. The sparse form composition approach encodes tumor areas into a low-redundancy representation, highlighting discriminative shape signals while minimizing noise and extraneous features. This encoding generates a concise feature set that emphasizes the morphological differences between tumor and healthy tissue. The collected sparse shape features are input into an NMSVM classifier.

This classifier is designed to address class imbalance and enhance differentiation between tumor and non-tumor areas. The system achieves great diagnostic accuracy by integrating shape-aware features with a strong decision boundary formulation. The integrated pipeline provides that segmentation precision immediately enhances classification efficacy. The proposed NMLR-SSC system shows resilience by efficiently managing noise via sparse encoding, addressing inter-patient anatomical variability via multilevel decomposition, and identifying lesions of varying sizes. Its consistency across clinical settings ensures dependable liver cancer classification, reducing performance degradation and improving real-world diagnostic relevance.

2.5. Performance analysis

The performance analysis section deliberates the investigation outcomes of the introduced NMSVM approach regarding true negative (TN), accuracy, specificity, true positive (TP), sensitivity, false negative (FN), false positive (FP), recall, precision, Dice, Jaccard, and Kappa coefficients. TP, FN, TN, FP parameters are utilized to classify the tumor as normal or any other abnormalities present in the liver. It correctly identifies the tumor portions in the liver organs effectively and these parameters are specified as shown in (10) to (14).

$$Sensitivity = \frac{TP}{TP+FN} \tag{10}$$

$$Specificity = \frac{TN}{TN+FP} \tag{11}$$

$$Accuracy = \frac{TP+TN}{P+N} \; or \; \frac{TP+TN}{TP+TN+FP+FN} \tag{12}$$

$$Precision = \frac{TP}{TP+FP} \tag{13}$$

$$Recall = \frac{TP}{TP+FN} \tag{14}$$

- F-measure: the F-measure is defined as calculating the test's accuracy and is otherwise stated as the weighted arithmetic mean of precision and recall.
- Jaccard coefficient: the coefficient is calculated as in (15).

$$JC_{ij} = \frac{a}{a+b+c} \tag{15}$$

- Dice coefficient: Dice coefficient is given by (16).

$$DC = 2\frac{precision*recall}{Precision+recall} \tag{16}$$

- Kappa coefficient as in (17).

$$KC = \frac{R_o - R_e}{1-P_e} \tag{17}$$

- Global acceptance rate as in (18).

$$100 - FRR \tag{18}$$

Figure 2 explains the training and testing images. Figure 2(a) shows an original abdominal CT image, Figure 2(b) describes the shape sharpening image, Figure 2(c) explains liver segmentation without tumor region, Figure 2(d) shows the liver segmented image, Figure 2(e) explains tumor identification, and Figure 2(f) indicates the tumor extraction region. Here, 409 images have been taken for training and testing. They have split into 70% and 30% of the training and the testing images are considered. Figure 3 depicts the image processing in accordance with the three kinds of disease conditions of liver tumor stage A, B, and C. Figure 4 presents images of shape reconstruction that demonstrate the retention of tumor geometry. Original masks reveal authentic areas, smoothed reconstructions enhance borders, and sparse reconstructions emphasize critical structural attributes, illustrating the model's precise tumor shape representation for categorization.

Figure 5 shows that the proposed NMSVM classifier achieves greater performance results than the probabilistic neural network (PNN) and k-nearest neighbors (KNN) classifiers. The sensitivity improved by 0.22%, and the accuracy by 3% in PNN and 8% in KNN. Hence, the proposed NMSVM attains 100% specificity, sensitivity, and a 98% accuracy rate. Figure 6 shows that the recall rate of the proposed NMSVM classifier improves by 22% more than the KNN classifier, and the F-measure range improves by 12.7% more than the KNN classifier. False acceptance rate (FAR), Figure 7 represents the FAR measures. Here, the NMSVM classifier accepts the fault instances. It shows 100% effective results than the existing techniques. False rejection rate (FRR) is the process of calculating the measurement of genuine consumers disallowed through the security method. Figure 8 represents the FRR measures. From Figures 6 and 7, the proposed NMSVM classifier rejects the faults effectively. Hence, the proposed NMSVM classifier accomplishes better results than the existing PNN and KNN classifiers.

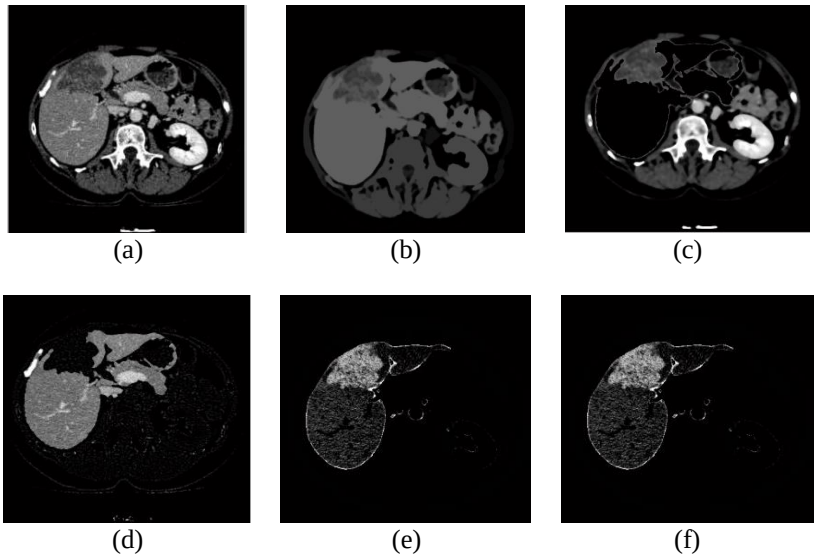

Figure 2. Training and testing images of (a) original abdominal CT images, (b) shape sharpening image, (c) liver segmented without tumor region, (d) liver segmented image, (e) tumor identification, and (f) tumor extraction region

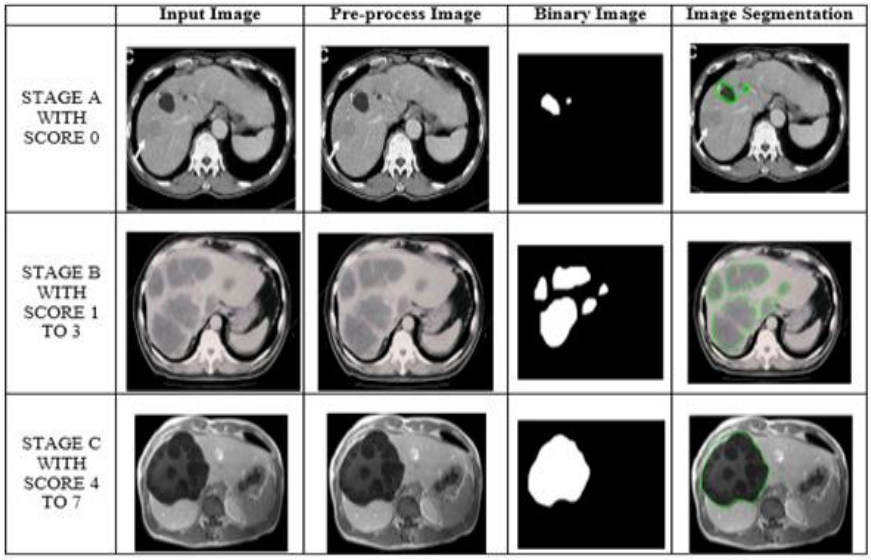

Figure 3. Image processing in accordance with the three kinds of disease conditions of liver tumor stage A, B, and C

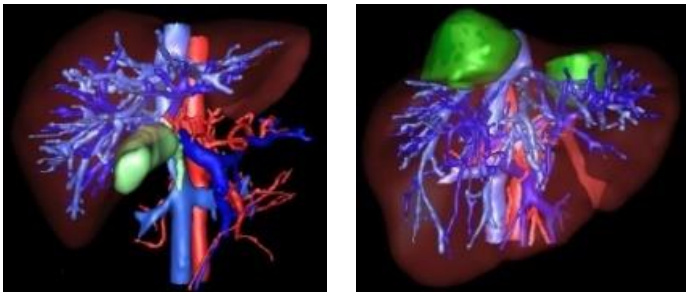

Figure 4. Liver tumor shape reconstruction samples

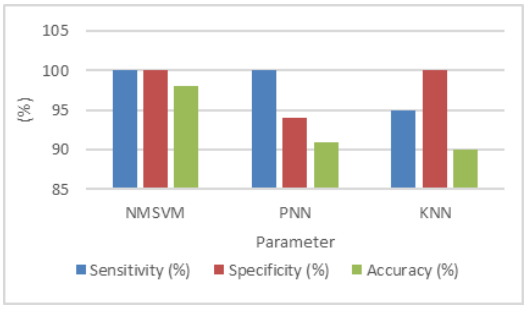

Figure 5. Sensitivity, specificity, and accuracy

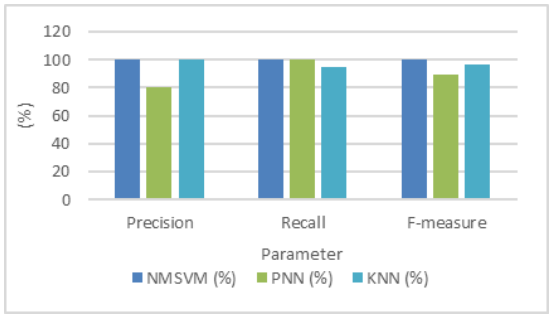

Figure 6. Precision, recall, and F-measure

Figure 7. False acceptance rate analysis

Figure 8. False rejection rate analysis

3. DISCUSSION

Today, liver cancer is very common, and hence, tumor detection in its earlier stage is more significant. A masking operation was used to eradicate the unwanted regions and was utilized for further processing without modifying any structure or shape. A high value means the condition is severe. Table 1 describes the hybrid statistical features in accordance with mean, variance, kurtosis, and skewness. Figure 9 depicts the receiver operating characteristic (ROC) curves of the proposed and the existing system. Tenfold cross-validation: the subsequent table offers a detailed description of the tenfold cross-validation of the proposed and existing classifiers. Figure 10 depicts classifier performance, demonstrating that NMSVM achieves higher accuracy, precision, and specificity relative to FLAS-U-Net++ and ResU-Net, highlighting its resilience and clinical dependability in liver tumor diagnosis.

Table 2 compares NMSVM, PNN, and KNN, indicating that NMSVM achieves higher accuracy, sensitivity, specificity, F1-score, Dice coefficient, and area under the curve (AUC) for dependable liver tumor identification. The analysis indicates that the proposed NMSVM outperforms FLAS-U-Net++ and ResU-Net, achieving high performance. This illustrates its efficacy in liver tumor identification, reducing false positives and facilitating dependable clinical decision-making in early cancer diagnosis. The NMLR-SSC framework is resource-intensive, necessitating graphics processing unit (GPU) acceleration or optimization for real-time implementation. The generalization to unknown lesion types remains untested, and integrating it into clinical workflows necessitates user-friendly interfaces, interoperability with picture archiving and communication system (PACS) systems, and validation against radiologist assessments, which may be limited without comprehensive user-centered design and regulatory approval. The NMLR-SSC + NMSVM framework is an innovative instrument that facilitates the early identification of liver cancer by precisely detecting tiny and diverse lesions. It may be integrated with PACS systems, radiological reporting tools, and hospital artificial intelligence (AI) platforms, enhancing process adoption and assisting radiologists in decision-making.

Table 1. The hybrid statistical features

Scores	Mean	Variance	Skewness	Kurtosis
Score 0	11.75143	4691.613	11.75143	8.751434
Score 1	13.51978	5397.62	13.51978	10.51978
Score 2	16.13809	6456.004	16.13809	13.13809
Score 3	16.1889	6498.528	16.1889	13.1889
Score 4	17.89641	7195.907	17.89641	14.89641
Score 5	18.17006	7305.604	18.17006	15.17006
Score 6	18.40869	7342.431	18.40869	15.40869
Score 7	18.53426	7406.646	18.53426	15.53426

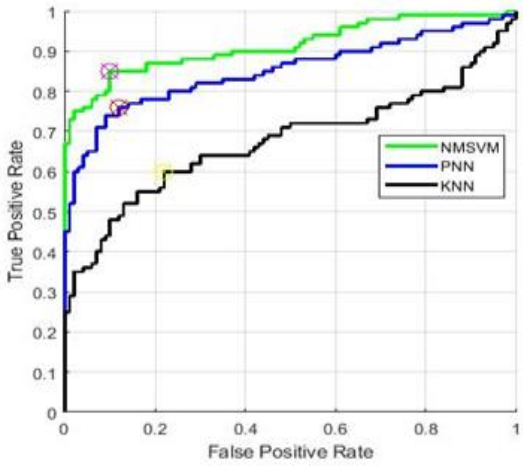

Figure 9. ROC curves for the existing and proposed systems

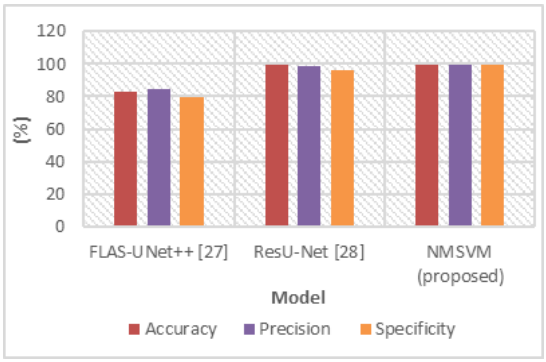

Figure 10. Classifier performance comparison

Table 2. Comparative performance of NMSVM, PNN, and KNN classifiers

Classifier	Accuracy (%)	Sensitivity (%)	Specificity (%)	F1-score	Dice coefficient	AUC
NMSVM	99.39	99.61	99.13	0.9942	0.9885	0.9961
PNN	98.98	98.42	99.58	0.9901	0.9803	0.9842
KNN	98.78	98.33	99.21	0.9874	0.9752	0.9833

4. CONCLUSION AND FUTURE WORK

This study introduces an NMSVM classifier that is trained using statistical texture data. It can distinguish between benign tumors, which have a classification of 0, and malignant tumors, which range from 1 to 7 values. A combination of statistical features with generalized linear model (GLM) features gives a hybrid HSGLCM approach, which is used for the objective of removing features from the input image. This novel technique is the primary driver of improved classification accuracy above current technologies. Only the pertinent values of the statistical features are extracted and further classified. This extraction procedure effectively separates the tumor-detected regions in the liver image and is mainly enhanced by the NMLR-SSC model. Compared to the current PNN and KNN classifiers, the proposed NMSVM approach performed better. Therefore, the accuracy of the proposed NMSVM classifier was 98%, and it outperformed the current PNN and KNN classifiers by 7% and 8%, respectively.

FUNDING INFORMATION

Authors state no funding involved.

AUTHOR CONTRIBUTIONS STATEMENT

This journal uses the Contributor Roles Taxonomy (CRediT) to recognize individual author contributions, reduce authorship disputes, and facilitate collaboration.

Name of Author	C	M	So	Va	Fo	I	R	D	O	E	Vi	Su	P	Fu
Balasubramanian Sakthisaravanan	✓	✓	✓			✓	✓		✓	✓				✓
Ramakrishnan Meenakshi	✓	✓	✓	✓		✓	✓			✓	✓	✓	✓	✓
Thirugnanasambandam Akila		✓		✓	✓		✓	✓	✓	✓		✓	✓	✓
Saravanan Durga Devi	✓		✓	✓	✓	✓		✓		✓	✓	✓	✓	
Subbiah Murugan	✓				✓	✓				✓		✓		✓

C : **C**onceptualization
M : **M**ethodology
So : **So**ftware
Va : **Va**lidation
Fo : **Fo**rmal analysis
I : **I**nvestigation
R : **R**esources
D : **D**ata Curation
O : Writing - **O**riginal Draft
E : Writing - Review & **E**diting
Vi : **Vi**sualization
Su : **Su**pervision
P : **P**roject administration
Fu : **Fu**nding acquisition

CONFLICT OF INTEREST STATEMENT

Authors state no conflict of interest.

DATA AVAILABILITY

The authors confirm that the data supporting the findings of this study are available within the article [and/or its supplementary materials].

REFERENCES

[1] Y. N. Gowda and R. V. Manjunath, "Automatic liver tumor classification using U-Net70 a deep learning model," *Journal of Liver Transplantation*, vol. 18, May 2025, doi: 10.1016/j.liver.2025.100260.
[2] S. Zhen *et al.*, "Deep learning for accurate diagnosis of liver tumor based on magnetic resonance imaging and clinical data," *Frontiers in Oncology*, vol. 10, May 2020, doi: 10.3389/fonc.2020.00680.
[3] V. R. Kavitha, F. B. J. Hussain, P. Chillakuru, and P. Shanmugam, "Automated classification of liver cancer stages using deep learning on histopathological images," *Traitement du Signal*, vol. 41, no. 1, pp. 373–381, Feb. 2024, doi: 10.18280/ts.410131.
[4] N. Mohankumar *et al.*, "Advancing chronic pain relief cloud-based remote management with machine learning in healthcare," *Indonesian Journal of Electrical Engineering and Computer Science*, vol. 37, no. 2, Feb. 2025, doi: 10.11591/ijeecs.v37.i2.pp1042-1052.

[5] H. Lv, H. Chen, S. Sun, Z. Mao, and G. Wang, "Optimization of tissue temperature field in tumor laser thermal therapy based on step response model and particle swarm optimization algorithm," *Journal of Thermal Biology*, vol. 139, Jul. 2026, doi: 10.1016/j.jtherbio.2026.104488.
[6] L. Qiu *et al.*, "Artificial intelligence-enhanced Couinaud segmentation for precision liver cancer therapy," *Biomedical Signal Processing and Control*, vol. 120, Jul. 2026, doi: 10.1016/j.bspc.2026.110100.
[7] H. Shin *et al.*, "Deep learning-based liver tumor segmentation from computed tomography scans with a gradient-enhanced network," *Diagnostics*, vol. 16, no. 3, Feb. 2026, doi: 10.3390/diagnostics16030429.
[8] V. S. D. Tejaswi and V. Rachapudi, "Liver cancer classification via deep hybrid model from CT image with improved texture feature set and fuzzy clustering based segmentation," *Web Intelligence*, vol. 22, no. 3, pp. 291–314, Sep. 2024, doi: 10.3233/WEB-230042.
[9] P. Maheswari, S. Gowriswari, S. Balasubramani, A. R. Babu, J. NK, and S. Murugan, "Intelligent headlights for adapting beam patterns with raspberry pi and convolutional neural networks," in *2024 2nd International Conference on Device Intelligence, Computing and Communication Technologies*, Mar. 2024, pp. 182–187, doi: 10.1109/DICCT61038.2024.10533159.
[10] F. I. Mir, G. Raj, K. Lata, A. S. Verma, and S. Ali, "Analysis for liver tumor segmentation using hybrid deep learning," in *Artificial Intelligence and Sustainable Innovation*, Boca Raton, United States: CRC Press, 2025, pp. 290–297, doi: 10.1201/9781003731689-43.
[11] R. Kılıç, A. Yalçın, F. Alper, E. A. Oral, and I. Y. Ozbek, "Two-stage automatic liver classification system based on deep learning approach using CT images," *Journal of Imaging Informatics in Medicine*, vol. 39, no. 1, pp. 311–333, May 2025, doi: 10.1007/s10278-025-01480-z.
[12] T. Sumallika and R. S. Prasad, "LiverScope: an automated deep classification of liver cancer detection," in *2025 6th International Conference on Mobile Computing and Sustainable Informatics*, Jan. 2025, pp. 1669–1673, doi: 10.1109/ICMCSI64620.2025.10883361.
[13] B. J. Ganesh, P. Vijayan, V. Vaidehi, S. Murugan, R. Meenakshi, and M. Rajmohan, "SVM-based predictive modeling of drowsiness in hospital staff for occupational safety solution via IoT infrastructure," in *2024 2nd International Conference on Computer, Communication and Control*, Feb. 2024, pp. 1–5, doi: 10.1109/IC457434.2024.10486429.
[14] M. D. A. Hasan, K. Balasubadra, G. Vadivel, N. Arunfred, M. V. Ishwarya, and S. Murugan, "IoT-driven image recognition for microplastic analysis in water systems using convolutional neural networks," in *2024 2nd International Conference on Computer, Communication and Control*, Feb. 2024, pp. 1–6, doi: 10.1109/IC457434.2024.10486490.
[15] S. Muhammad and J. Zhang, "Segmentation of liver tumors by Monai and PyTorch in CT images with deep learning techniques," *Applied Sciences*, vol. 14, no. 12, Jun. 2024, doi: 10.3390/app14125144.
[16] K. Padmanaban, A. M. S. Kumar, H. Azath, A. K. Velmurugan, and M. Subbiah, "Hybrid data mining technique based breast cancer prediction," in *AIP Conference Proceedings*, 2023, doi: 10.1063/5.0110216.
[17] S. Narasimhulu and C. D. V. S. Rao, "Liver tumor segmentation and classification using deep learning methods," in *2024 International Conference on Distributed Computing and Optimization Techniques*, Mar. 2024, pp. 1–5, doi: 10.1109/ICDCOT61034.2024.10515854.
[18] S. Dharaneswar and B. P. S. Kumar, "Liver tumor diagnosis using trans-dense R2U-Net++ segmentation and pyramid dilated adaptive residual deep learning-based classification technique," *Sensing and Imaging*, vol. 27, no. 1, Feb. 2026, doi: 10.1007/s11220-025-00691-6.
[19] N. Mizouri, "Deep learning neural network with transfer learning for liver cancer classification," *Medinformatics*, 2025, doi: 10.47852/bonviewmedin52025652.
[20] S. S. Roy, S. Roy, P. Mukherjee, and A. H. Roy, "An automated liver tumor segmentation and classification model by deep learning based approaches," *Computer Methods in Biomechanics and Biomedical Engineering: Imaging & Visualization*, vol. 11, no. 3, pp. 638–650, 2023, doi: 10.1080/21681163.2022.2099300.
[21] S. C. Lingamaiah, T. B. Krishna, A. K. R. Poreddy, and P. Kokil, "Attention-based deep learning model for clinical assessment of focal liver lesions using ultrasound imaging," *Biomedical Signal Processing and Control*, vol. 116, May 2026, doi: 10.1016/j.bspc.2026.109563.
[22] P. Dhanalakshmi, S. Tarun, R. R. Dasari, S. Purushotham, and P. Lehitha, "A graph neural network framework for colorectal liver metastasis tumor burden evaluation," *Proceedings of 9th International Conference on Inventive Computation Technologies (ICICT 2026)*, pp. 1488–1493, 2026, doi: 10.1109/ICICT68280.2026.11510822.
[23] L. N. Mahdy, K. A. Ezzat, M. Torad, and A. E. Hassanien, "Automatic segmentation system for liver tumors based on the multilevel thresholding and electromagnetism optimization algorithm," *International Journal of Imaging Systems and Technology*, vol. 30, no. 4, pp. 1256–1270, Dec. 2020, doi: 10.1002/ima.22432.
[24] B. Karabağ, K. Ayturan, and F. Hardalaç, "Liver tumor segmentation with deep learning: a comparative analysis of CNN-, transformer-, and YOLO-based models on the ATLAS MRI," *Diagnostics*, vol. 16, no. 5, 2026, doi: 10.3390/diagnostics16050649.
[25] S. Srinivasan, G. Indra, T. R. Saravanan, S. Murugan, C. Srinivasan and M. Muthulekshmi, "Revolutionizing skin cancer detection with Raspberry Pi-embedded ANN technology in an automated screening booth, " in *4th International Conference on Innovative Practices in Technology and Management*, 2024, pp. 1-6, doi: 10.1109/ICIPTM59628.2024.10563383.

BIOGRAPHIES OF AUTHORS

Balasubramanian Sakthisaravanan received his B.Tech. degree in Information Technology (First class) from Saveetha Engineering College (affiliated to Anna University), Chennai, India, in 2008, and the M.Tech. degree in Information Technology (First Class) from Sathyabama University, Chennai, India, in 2012 (First Class). He completed his Ph.D. degree in "Liver tumor segmentation and classification using outline preservation and multilevel local region-based sparse shape composition method" from Saveetha University, Chennai, India (2023). Currently, he is working as a professor in the Department of Computer Science and Engineering, Sri Venkateshwara College of Engineering, Bengaluru, India. His research interests include image processing and networking. He is a life member of professional bodies like UACEE, CSTA, ACM, IAENG, and ICST. He can be contacted at email: sakthisaravanan.b_cy@svcengg.edu.in or saravanansakthisaravanan582@gmail.com.

Dr. Ramakrishnan Meenakshi received her M.Tech. degree in Computer Science (First class with Distinction) from SRM University, Chennai, India, in 2005. She completed her Ph.D. degree in "Brain tumor classification using orthogonal polynomial-based composite operators for MRI" from Anna University (2014). Currently, she is working as a professor in the Department of Computer Science and Engineering, Chennai Institute of Technology, Chennai, India. Her research interests include image processing and wireless networking. She is a life member of professional bodies like CSI, UACEE, CSTA, IAENG, IAOE, SDIWC. She can be contacted at email: meenakshir@citchennai.net.

Thirugnanasambandam Akila is an associate professor in the Department of Information Technology, Mahendra College of Engineering, Salem, India, with 20 years of teaching experience. She graduated with an M.E. from VMRF Deemed University. She has completed a Ph.D. from Anna University. Her main research interests are computer networks, wireless communication, and wireless sensor networks. Apart from these, her research interests also include artificial intelligence, web information retrieval, and natural language processing, text mining, specifically the application of statistical and NLP techniques in big data, machine learning, and DL. Her research contributions have culminated in 25 publications, including international journals and international conferences, and national conferences. She can be contacted at akilat.cse@gmail.com.

Dr. Saravanan Durga Devi is an associate professor in the Department of Computer Science and Engineering at Vel Tech High Tech Dr. Rangarajan Dr. Sakunthala Engineering College, Chennai, India. Her area of interest is network security, wireless systems, and IoT. She has vast experience in academia and administration. She has published and presented papers in various international and national journals/conferences. She is an active member of professional bodies, CSI, and ISTE. She can be contacted at email: sdurgadevi@velhightech.com.

Dr. Subbiah Murugan is an adjunct professor, Department of Biomedical Engineering, Saveetha School of Engineering, Saveetha Institute of Medical and Technical Sciences, Saveetha University, Chennai, India. He has published his research articles in many international and national conferences and journals. His research areas include network security and machine learning. He can be contacted at email: smuresjur@gmail.com.